

Ammonia movement and distribution after exercise across white muscle cell membranes in rainbow trout

Y. Wang, G. J. Heigenhauser and C. M. Wood

Am J Physiol Regul Integr Comp Physiol 271:738-750, 1996.

You might find this additional information useful...

This article has been cited by 2 other HighWire hosted articles:

Effects of sublethal ammonia exposure on swimming performance in rainbow trout (*Oncorhynchus mykiss*)

A. Shingles, D. J. McKenzie, E. W. Taylor, A. Moretti, P. J. Butler and S. Ceradini
J. Exp. Biol., January 8, 2001; 204 (15): 2691-2698.

[\[Abstract\]](#) [\[Full Text\]](#) [\[PDF\]](#)

Respiratory and metabolic functions of carbonic anhydrase in exercised white muscle of trout

Y. Wang, R. P. Henry, P. M. Wright, G. J. F. Heigenhauser and C. M. Wood
Am J Physiol Regulatory Integrative Comp Physiol, December 1, 1998; 275 (6): R1766-1779.

[\[Abstract\]](#) [\[Full Text\]](#)

Medline items on this article's topics can be found at

<http://highwire.stanford.edu/lists/artbytopic.dtl>

on the following topics:

- Physiology .. Salmoniformes
- Physiology .. Muscle Cell
- Physiology .. Exertion
- Medicine .. Behavioral and Psychosocial Issues
- Medicine .. Fitness (Physical Activity)
- Medicine .. Exercise

Additional material and information about *American Journal of Physiology - Regulatory, Integrative and Comparative Physiology* can be found at:

<http://www.the-aps.org/publications/ajpregu>

This information is current as of April 28, 2006 .

Ammonia movement and distribution after exercise across white muscle cell membranes in rainbow trout

YUXIANG WANG, GEORGE J. F. HEIGENHAUSER, AND CHRIS M. WOOD
Department of Biology and Department of Medicine,
McMaster University, Hamilton, Ontario L8S 4K1, Canada

Wang, Yuxiang, George J. F. Heigenhauser, and Chris M. Wood. Ammonia movement and distribution after exercise across white muscle cell membranes in rainbow trout. *Am. J. Physiol.* 271 (Regulatory Integrative Comp. Physiol. 40): R738–R750, 1996.—Manipulations of pH and electrical gradients in a perfused preparation were used to analyze the factors controlling ammonia distribution and flux in trout white muscle after exercise. Trout were exercised to exhaustion, and then an isolated-perfused white muscle preparation with discrete arterial inflow and venous outflow was made from the posterior portion of the tail. The tail-trunks were perfused with low (7.4)-, medium (7.9)-, and high (8.4)-pH saline, achieved by varying HCO_3^- concentration ($[\text{HCO}_3^-]$) at constant PCO_2 . Intracellular and extracellular pH, ammonia, CO_2 , K^+ , Na^+ , and Cl^- were measured. Muscle intracellular pH was not affected by changes in extracellular pH. Increasing extracellular pH caused a decrease in the transmembrane NH_3 partial pressure (P_{NH_3}) gradient and a decrease in ammonia efflux. When extracellular K^+ concentration was increased from 3.5 to 15 mM in the medium-pH group, a depolarization of the muscle cell membrane potential from -92 to -60 mV and a 0.1-unit depression in intracellular pH occurred. Ammonia efflux increased despite a marked reduction in the P_{NH_3} gradient. Amiloride (10^{-4} M) had no effect, indicating that $\text{Na}^+/\text{H}^+-\text{NH}_4^+$ exchange does not participate in ammonia transport in this system. A comparison of observed intracellular-to-extracellular ammonia distribution ratios with those modeled according to either pH or Nernst potential distributions supports a model in which ammonia distribution across white muscle cell membranes is affected by both pH and electrical gradients, indicating that the membranes are permeable to both NH_3 and NH_4^+ . Membrane potential, acting to retain high levels of NH_4^+ in the intracellular compartment, appears to have the dominant influence during the postexercise period. However, at rest, the pH gradient may be more important, resulting in much lower intracellular ammonia levels and distribution ratios. We speculate that the muscle cell membrane NH_3 -to- NH_4^+ permeability ratio in trout may change between the rest and postexercise condition.

trout muscle; NH_3 ; NH_4^+ ; intracellular pH; extracellular pH; Nernst potential

branes, exclusively by water-filled channels. However, NH_4^+ is much more plentiful than NH_3 and may also move by various carrier-mediated mechanisms (e.g., substitution into Na^+/H^+ exchangers; see Ref. 1).

Ammonia is the major end product of nitrogen metabolism ($>70\%$) in ammoniotelic animals such as teleost fish. At rest, most ammonia is produced by transamination and deamination of amino acids in the liver (see Ref. 34 for review), but, during exhaustive exercise and hypoxia, large additional amounts of ammonia are produced in white muscle through the deamination of adenylates as ATP stores are degraded (6, 19, 25, 29). In mammals, ATP stores are defended and intracellular and extracellular ammonia levels remain relatively low (9, 15, 20), but in exercising fish muscle, ammonia production is sufficient to serve as an important intracellular buffer of the accompanying lacticidosis, as well as an important modulator of glycolytic flux at the level of phosphofructokinase (6). Furthermore, most of the ammonia produced appears to be retained in the muscle cells, together with inosine monophosphate, so as to fuel later resynthesis of the adenylate pool in fish (19, 29).

In mammals, ammonia movement and distribution across muscle cell membranes traditionally follow the theory of nonionic diffusion (20); i.e., ammonia moves as NH_3 according to NH_3 partial pressure (P_{NH_3}) gradients and therefore distributes according to transmembrane pH gradients, because NH_3 permeability (P_{NH_3}) is so much higher than NH_4^+ permeability ($P_{\text{NH}_4^+}$; 13, 17). As illustrated in Fig. 1A, this will lead to distribution ratios (intracellular to extracellular) of ~ 4.0 . However, several recent studies have questioned this hypothesis because of the finding of significant disagreement between the measured muscle-to-plasma distribution ratio for ammonia and that predicted by the pH gradient (9, 10). In fish muscle, the situation is also unclear (24, 34). Most experimental studies (27, 29, 38, 39), but not all (19), have indicated that intracellular ammonia levels after exercise are far higher than explicable by a pH-driven distribution, but very close to those predicted by a Nernst distribution between intracellular (ICF) and extracellular fluid (ECF), assuming a muscle cell membrane potential (E_m) in the range of -80 to -100 mV. As illustrated in Fig. 1B, this will result in a distribution ratio of ~ 30.0 . These studies suggest that the influence of E_m on NH_4^+ is the dominant factor governing transmembrane distribution, so that $P_{\text{NH}_4^+}$ must be appreciable. However, this concept has been strongly criticized on theoretical grounds (11), most notably because an “ NH_4^+ shuttle” could result in an inwardly directed flux of H^+ into the cells (38), creating an intolerable load for the intracellular pH (pH_i) regula-

AMMONIA IS A RESPIRATORY gas that behaves as a weak electrolyte in solution (13, 17). With a pK of 9.0–10 under physiological conditions, $>95\%$ exists as NH_4^+ and the remainder as NH_3 (4). Whereas NH_3 is often considered to be highly lipophilic, available data indicate that this is not the case and that the lipid versus water partition coefficient is <0.1 (7). Diffusion through water-filled channels is likely to be much faster than diffusion through lipoprotein bilayers. NH_4^+ is charged and larger in ionic radius, especially in the hydrated form, and likely diffuses more slowly across cell mem-

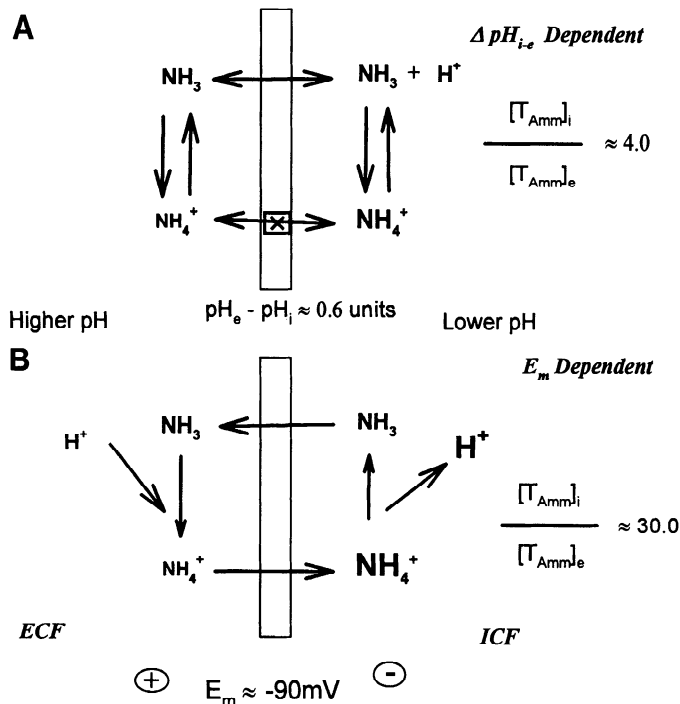


Fig. 1. Schematic models of ammonia transport and distribution across muscle cell membrane. *A*: scenario when membrane is only permeable to NH_3 . *B*: scenario when membrane also has a significant permeability to NH_4^+ . Note very different distribution ratios that result. ΔpH_{i-e} , change in intracellular to extracellular pH; $[T_{Amm}]_i$, $[T_{Amm}]_e$, concentrations of intracellular and extracellular total ammonia, respectively; E_m , membrane potential; ICF, ECF, intra- and extracellular fluid, respectively.

tory mechanisms of the cell (Fig. 1*B*). The situation is further complicated by the finding of Tang et al. (27) on postexercise trout in vivo that, despite an ammonia distribution between ICF and ECF apparently in accord with E_m , experimentally increasing the extracellular pH (pH_e)- pH_i gradient by bicarbonate infusion resulted in a greater apparent retention of ammonia in white muscle. Our own recent in vivo study on trout muscle (29) indicated that ammonia distribution might change from a distribution governed by the pH gradient at rest to a distribution governed by E_m after exercise, in contrast to an earlier study showing an E_m -driven distribution under both circumstances (39).

In light of these uncertainties, the present study concentrates on the postexercise situation and employs a perfused rainbow trout tail-trunk preparation that has been naturally loaded with ammonia via exercise-induced adenylate breakdown (6, 27, 29, 39). In the present report, the preparation is characterized and then used to examine the factors governing transmembrane ammonia distribution and flux in rainbow trout white muscle. Parallel studies with this preparation have examined the factors governing transmembrane lactate, metabolic acid, bicarbonate, and CO_2 distribution and flux (Wang et al., unpublished results). The approach eliminates many of the uncertainties associated with in vivo studies. In particular, the preparation allowed us to measure both the efflux to the perfusate and the transmembrane distribution with respect to

the venous side. Previous in vivo studies have not been able to monitor efflux and may have overestimated ICF-to-ECF distribution ratios because only arterial ECF samples were obtained. Furthermore, the preparation allowed us to manipulate the pH and electrical gradients between ECF and ICF. Extracellular bicarbonate levels were varied to alter pH_i - pH_e , high-ECF potassium was used to partially depolarize the muscle cell E_m , and amiloride (1) was employed to block the possible involvement of $Na^+/H^+-NH_4^+$ carriers.

MATERIALS AND METHODS

Experimental Animals

Rainbow trout (500–600 g) were obtained from Spring Valley Trout Farm (Petersburg, Ontario) and then raised for 2–6 mo in a 800-liter fiberglass cylindrical tank with flowing dechlorinated Hamilton tap water (in meq/l: 0.6 Na^+ , 0.8 Cl^- , 1.8 Ca^{2+} , 0.5 Mg^{2+} , 0.04 K^+ ; pH 8.0, temperature 5–12°C) until the desired size (800–1,000 g) was reached. During this period the fish were fed with high-protein trout grower floating pellets (Aquaculture Zeigler Brothers) three times a week. Before the experiment, fish were acclimated to $15 \pm 1^\circ C$ for 5–7 days without feeding to standardize metabolic status. Exercised fish were used in this perfusion study to elevate muscle ammonia levels that naturally occur via adenylate breakdown. Before perfusion, the fish were manually chased for 6 min to exhaustion in a 150-liter cylindrical tank (29). Immediately on cessation of exercise, the trout was transferred to a dark acrylic box containing 8 liters aerated water and anesthetized with MS-222 (0.5 g/l neutralized with NaOH). This resulted in loss of equilibrium and cessation of ventilation within 1 min without struggling. This method has been proven to cause minimum metabolic and acid-base disturbances (26, 30). The tail was cut off at the level of the anus and weighed before perfusion. The unconscious fish was killed immediately after the tail was removed.

Experimental Protocols

Experimental design and perfusate preparation. This study was designed to investigate how changes in pH and electrical gradients between ICF and ECF of muscle affect transmembrane ammonia flux and distribution. Cortland salmonid saline with 3% bovine serum albumin (BSA; fraction V, Sigma) was used as the basic perfusate. Ammonia already present in the distilled water and component salts was sufficient to provide normal resting arterial levels of total ammonia (T_{Amm} ; $\sim 50 \mu mol/l$) in the perfusate (27, 29, 30, 39). PCO_2 was kept constant at ~ 2 Torr to represent the typical resting value of trout arterial blood in vivo (29). $NaHCO_3$ levels were adjusted accordingly to manipulate perfusate pH_e in different treatment groups (Table 1). Changes in the pH gradient were achieved by altering perfusate pH_e while the electrical gradient was depressed by elevating perfusate potassium concentration ($[K^+]$) from the normal level of

Table 1. Expected inflow saline pH, PCO_2 , HCO_3^- , and K^+ in the four experimental treatment groups

| Treatment Groups | pH | PCO_2 , Torr | HCO_3^- , mM | K^+ , mM |
|--------------------------|-----|----------------|----------------|------------|
| Low pH | 7.4 | 2 | 2 | 3 |
| Medium pH (control) | 7.9 | 2 | 7 | 3 |
| High pH | 8.4 | 2 | 18 | 3 |
| High K^+ (depolarized) | 7.9 | 2 | 7 | 15 |

~3–15 mM (high K^+). The study comprises four treatment groups (6–11 fish per group): low, medium, and high pH_e and high potassium (at medium pH_e), as shown in Table 1. The medium- pH_e group was used as the control group, with normal $pH_e \approx 7.9$, which mimics resting trout arterial plasma pH (29). The low- pH_e group ($pH \approx 7.4$) simulates the typical trout arterial plasma pH after exhaustive exercise (29). The high- pH_e group ($pH \approx 8.4$) was chosen to create an elevated transmembrane pH gradient, which could occur under some circumstances such as high environmental pH (31). The pH and HCO_3^- concentration ($[HCO_3^-]$) of the high- K^+ group ($[K^+] \approx 15$ mM) were kept at the control level. Changes in saline $[HCO_3^-]$ were achieved by reciprocal changes in $NaHCO_3$ and NaCl so as to maintain Na^+ concentration ($[Na^+]$) constant in various treatment groups. However, in the high- K^+ group, because 12 mmol more KCl was added to elevate the perfusate K^+ level, the NaCl level was reduced correspondingly to avoid introducing excessive Cl^- into the saline.

On the basis of the results of these studies, it was apparent that one of the drug treatments used in our parallel study on lactate and metabolic acid transport in the perfused postexercise trunk preparation (Wang et al., unpublished results) could provide useful information on ammonia transport. Methods were identical to that of the low- pH_e treatment, except that 10^{-4} M amiloride HCl (Sigma) was present in the perfusate throughout the second 30 min of perfusion. Perfusate and tissue samples from these trunks ($n = 11$) were analyzed for all ammonia-relevant parameters; these data are presented in the current study.

Perfusion and sampling. Immediately after the tail trunk was severed from the body and weighed (10–15 s), catheters (Clay-Adams PE-90 tubing) were implanted to a depth of 1.5–2.0 cm into the caudal artery and caudal vein and secured by a ligation in a deep incision around the vertebral column. This deep insertion and ligation ensured that there was no leakage from the caudal vessels themselves and, furthermore, prevented perfusion of segmental arteries close to the plane of section, thereby minimizing leakage through the cut surface. With this technique, all of the venous outflowing perfusate that was collected from the caudal vein passed through the arterial-to-venous circuit of the preparation. Therefore, venous perfusate represented the true outcome of perfusion. The terminal muscle samples (see below) were also obtained from the area away from the cut surface where muscle tissue was fully perfused.

Perfusion was started immediately at $2 \text{ ml} \cdot \text{min}^{-1} \cdot 100 \text{ g}$ tail wt^{-1} with Cortland saline plus BSA of the appropriate pH and $[K^+]$. The saline was heparinized with 50 IU/ml sodium heparin (Sigma) to prevent blood clotting. The tail trunk was submerged in a temperature-controlled saline bath ($15 \pm 0.5^\circ\text{C}$) during the entire perfusion period, while the perfusate was pumped through a heat-exchange coil in a 15°C water bath. Sampling ports were placed in arterial and venous catheters to allow subsequent collection of inflowing and outflowing perfusate samples, respectively, and the outflow of the venous catheter was set to the level of the saline bath, i.e., zero pressure.

The perfusion preparation setup is shown schematically in Fig. 2. The perfusate was gassed with 0.25% CO_2 , balance O_2 , for at least 60 min in a Plexiglas disc oxygenator to achieve the desired pH, PO_2 and PCO_2 levels. Precision gas mixtures were supplied by Wöstoff gas-mixing pumps (Bochum, Germany) and saturated with water vapor before contact with the perfusate. The oxygenated perfusate was then drawn through the heat exchanger by a peristaltic pump (Gilson Minipuls 3) and delivered to the tail trunk via a windkessel to

dampen the pressure pulsatility. All tubing was stainless steel to minimize loss of O_2 and CO_2 . The perfusion rate was kept at $2 \text{ ml} \cdot \text{min}^{-1} \cdot 100 \text{ g}$ tail wt^{-1} throughout, approximately twice the blood perfusion rate in trout white muscle under exercise conditions in vivo (23, 32). The perfusion pressure was monitored by a transducer (Narco Bio-System RP-1500) and registered on a Gilson ICT-5H polygraph chart recorder. This initial perfusion lasted for 30 min to ensure washout of red blood cells.

At 30 min, arterial and venous perfusate samples (2 ml) were collected via the sampling ports with the use of a gas-tight Hamilton syringes. A second (final) set of perfusate samples was taken after a subsequent 30 min of perfusion with nonheparinized saline of the same composition. Venous samples of perfusate were drawn before the arterial samples to avoid the potential effect of the brief inflow interruption on the composition of the venous outflow sample. In fact, this was not a concern at 60 min because the arterial sample at this time was taken simultaneously with the termination of the experiment. At the 30-min sampling point, there was interruption of inflow, but the following 30 min of perfusion provided ample time for recovery.

Samples were analyzed for perfusate pH, PO_2 , total CO_2 (TCO_2), protein content, T_{Amm} , lactate (Lac), Cl^- , Na^+ , and K^+ . TCO_2 , pH, PO_2 , and protein content were measured immediately after sampling, while part of the perfusate sample (300 μl) was deproteinized with 8% perchloric acid (PCA, 600 μl), frozen in liquid N_2 , stored at -70°C , and neutralized before the later analysis of Lac. Perfusate ($\sim 500 \mu\text{l}$) was also frozen directly in liquid N_2 and stored at -70°C for analysis of T_{Amm} and electrolytes.

At the time when the tail was cut off, an initial muscle sample (3–5 g) was taken from the area between the lateral line and the dorsal fin immediately anterior to the point of section. A final muscle sample (3–5 g) was excised from the same position on the perfused tail-trunk (but away from the cut surface) after the second perfusate sample (i.e., at 60 min). On excision, the muscle samples were freeze-clamped within 5 s with aluminum tongs precooled in liquid N_2 and then stored in liquid N_2 . The muscle tissues were used to determine pH_i , TCO_2 , T_{Amm} , Lac, Cl^- , Na^+ , K^+ and H_2O content.

Analytic techniques. Frozen muscle tissue was ground to a fine powder in an insulated mortar and pestle cooled with liquid N_2 . Muscle pH_i was measured by the homogenization technique (22). One part of frozen tissue powder ($\sim 200 \text{ mg}$) was mixed with five parts of metabolic inhibitor (150 mmol/l potassium fluoride, 6 mmol/l sodium nitrilotriacetate, Sigma) in a 1.5-ml sealed centrifuge tube. The homogenate was then centrifuged at $9,000 g$ for 30 s, and the supernatant was used to measure muscle pH_i at 15°C with a Radiometer microelectrode (E5021) and PHM84 acid-base analyzer; muscle TCO_2 was also measured on this supernatant (Wang et al., unpublished results). Part of the powder ($\sim 100 \text{ mg}$) was extracted with 1 ml 8% PCA, and the supernatant of this tissue extract was used to analyze tissue T_{Amm} by the glutamate dehydrogenase method as modified by Kun and Kearney (14). The rest of the frozen tissue powder was lyophilized for 64 h and then stored in a freezer at -70°C for later measurement of Lac.

For measurement of ions, freeze-dried tissue powder (20 mg) was digested with 1 N ultrapure HNO_3 (1 ml) at 40 – 50°C for 48 h, and then the supernatant was used for Na^+ , K^+ , and Cl^- analyses. White muscle water content ($[\text{H}_2\text{O}]_i$) was determined by drying fresh tissue (0.5–1 g) to a constant weight at 80°C . Perfusate was also deproteinized with 1 N HNO_3 , and the supernatant was used for Na^+ and K^+

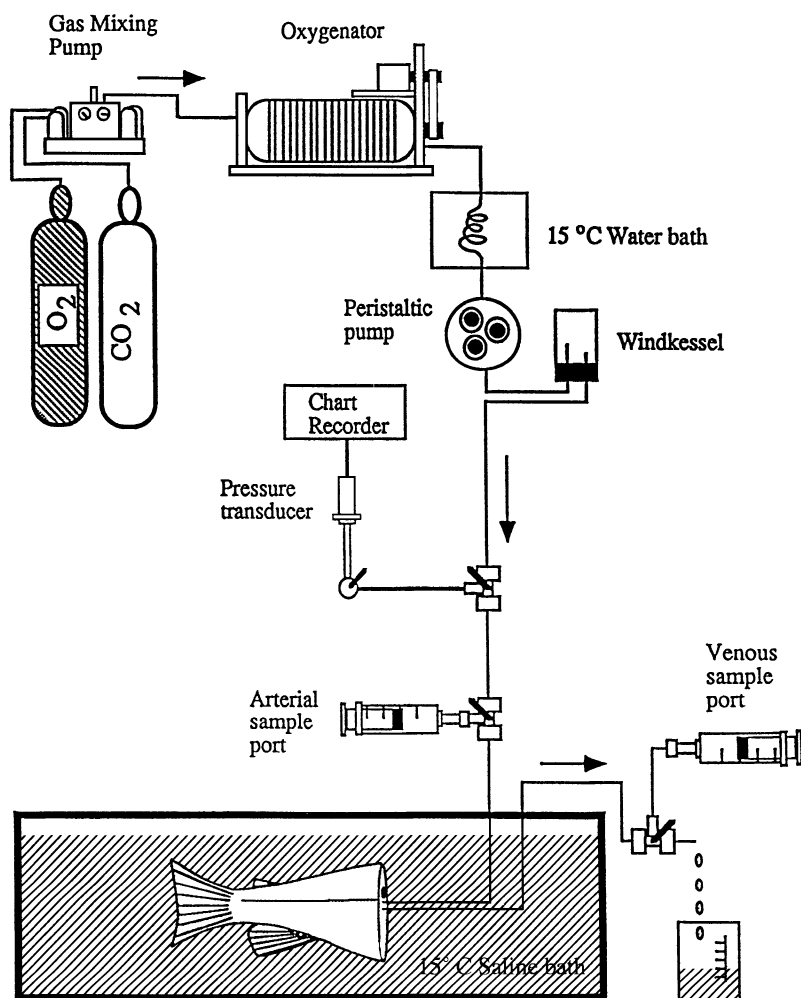


Fig. 2. Schematic diagram of isolated-perfused tail-trunk preparation of rainbow trout.

SDR Production

analysis. For perfusate Cl^- measurements, undiluted perfusate was used. Both Na^+ and K^+ were determined with flame atomic absorption spectrometry (Varian AA-1275), whereas Cl^- was analyzed by coulometric titration (Radiometer CMT10).

Perfusate pH was determined with the same acid-base apparatus used for muscle pH_i . Perfusate PO_2 was measured at 15°C with a Radiometer PO_2 electrode (E5046) connected to a Cameron Instrument OM-200 oxygen meter. Perfusate TCO_2 was determined on a Cameron Instrument Capni-Con total CO_2 analyzer (model II). PCO_2 and $[\text{HCO}_3^-]$ were calculated by manipulation of the Henderson-Hasselbalch equation using appropriate constants (αCO_2 and pK') for rainbow trout true plasma at 15°C (3). Total protein and water content of saline was measured with an American Optical refractometer.

The perfusate T_{Amm} content was measured by the glutamate dehydrogenase assay using a Sigma kit. Along with tissue T_{Amm} analysis, these enzymatic measurements were conducted on an LKB UltraspecPlus 4053 spectrophotometer.

Perfusate buffer capacity. The nonbicarbonate buffer capacities (β) of each of the four perfusates were determined. In brief, perfusate samples (4 ml) were placed in tonometer vessels (Instrumentation Laboratories 237) and equilibrated with 1, 2, 4, and 8 Torr PCO_2 , balance O_2 , for 20 min at 15°C ,

then analyzed for pH and TCO_2 with aforementioned methods. $[\text{HCO}_3^-]$ of the samples were calculated, and β in various treatment groups was determined from the slope of the regression of $[\text{HCO}_3^-]$ against pH

$$\beta = \frac{\Delta[\text{HCO}_3^-]}{\Delta\text{pH}} \quad (1)$$

Calculations and Statistics

The perfusion pressure has been expressed as net inflow pressure exerted on the tail trunks only, calculated as the difference between the perfusion pressure with and without the tail trunks in the system (i.e., correcting for cannula resistance). Inasmuch as the perfusion rate ($2 \text{ ml} \cdot 100 \text{ g tail wt}^{-1} \cdot \text{min}^{-1}$) was constant in each preparation, the perfusion pressure reflected the resistance of the tail trunk.

The ECF volume (ECFV, ml/g) and ICF volume (ICFV, ml/g) of white muscle in this perfusion preparation were estimated by $[\text{H}_2\text{O}]_t$ and Na^+ , K^+ , and Cl^- concentrations of the muscle and ECF (venous perfusate water in this case) using the "Cl $^-$ -K $^+$ space" approach of Conway (5)

$$\text{ICFV} = [\text{H}_2\text{O}]_t - \text{ECFV} \quad (2)$$

$$ECFV = \frac{[K^+]_t [Cl^-]_t - ([H_2O]_t)^2 [Cl^-]_e [K^+]_e}{[K^+]_t [Cl^-]_e + [Cl^-]_t [K^+]_e - 2 [H_2O]_t [Cl^-]_e [K^+]_e} \quad (3)$$

where the subscripted t and e are the concentrations in whole muscle tissue (mmol/kg for ions, ml/g for H_2O) and in ECF (mmol/l perfusate H_2O), respectively. The estimate of ECFV was made on the basis of the assumption that ions in ECF have been fully equilibrated with venous perfusate after 60 min of perfusion.

The ICF ions and T_{Amm} concentrations ($[S]_i$) were calculated as

$$[S]_i = \frac{[S]_t - [S]_e \times ECFV}{ECFV} \quad (4)$$

where the subscripted i is the concentration in ICF, and S represents ions or T_{Amm} .

Oxygen consumption (MO_2) and CO_2 efflux were calculated with the use of the Fick principle from the perfusion rate and the differences of gas content between inflow and outflow perfusate, e.g.

$$MO_2 (\text{mmol} \cdot \text{kg}^{-1} \cdot \text{h}^{-1}) = \text{perfusion rate} \times \alpha O_2 \times \Delta PO_2 \quad (5)$$

where ΔPO_2 is O_2 partial pressure difference between arterial and venous perfusate, and αO_2 ($1.77 \mu\text{mol} \cdot \text{l}^{-1} \cdot \text{Torr}^{-1}$) is the solubility coefficient of O_2 at 15°C in water of appropriate ionic strength to match the perfusate (3). An analogous equation, with the corresponding ΔTCO_2 values substituted for $\alpha O_2 \times \Delta PO_2$, was applied in the CO_2 efflux calculation.

Ammonia, as a metabolic substrate and an end product, exists as an anion, a respiratory gas, and a weak base ($pK \approx 9.7$ at 15°C). T_{Amm} is the sum of the ionic and nonionic forms of this substance

$$T_{Amm} = [NH_4^+] + [NH_3] \quad (6)$$

$$P_{NH_3} = \frac{[NH_3]}{\alpha NH_3} \quad (7)$$

where αNH_3 is taken from Cameron and Heisler (4).

At physiological pH (6.0–8.0), according to the following equation

$$pH = pK + \log \frac{[NH_3]}{[NH_4^+]} \quad (8)$$

over 98% of ammonia exists as NH_4^+ , with pK again from Cameron and Heisler (4). If the muscle cell membrane is permeable only to NH_3 and P_{NH_3} is in equilibrium across the membrane, then the total ammonia distribution will be a function of the transmembrane pH gradient only

$$\frac{[T_{Amm}]_{ICF}}{[T_{Amm}]_{ECF}} = \frac{1 + 10^{(pK - pH_i)}}{1 + 10^{(pK - pH_e)}} \quad (9)$$

Therefore, the relatively lower pH_i will trap more NH_4^+ in the ICF (Fig. 1A).

However, if the cell membrane is permeable only to NH_4^+ , ammonia will be distributed according to membrane Nernst potential (E_m) only

$$E_m = -\frac{RT}{ZF} \ln \frac{[NH_4^+]_i}{[NH_4^+]_e} = -\frac{RT}{ZF} \ln \frac{[T_{Amm}]_i - [NH_3]_i}{[T_{Amm}]_e - [NH_3]_e} \quad (10)$$

where R , T , Z , and F are the gas constant, the absolute temperature, the valence, and Faraday's constant, respectively. Under equilibrium conditions, the negatively charged

ICF will trap a great deal more NH_4^+ (Fig. 1B) than if pH were governing the distribution. The E_m of the white muscle was estimated from the measured intra- and extracellular concentrations of K^+ , Na^+ , and Cl^- according to the Goldman-Hodgkin-Katz equation

$$E_m = \frac{RT}{F} \ln \frac{PK^+ [K^+]_{ECF} + PNa^+ [Na^+]_{ECF} + PCl^- [Cl^-]_{ICF}}{PK^+ [K^+]_{ICF} + PNa^+ [Na^+]_{ICF} + PCl^- [Cl^-]_{ECF}} \quad (11)$$

where PK^+ , PNa^+ , and PCl^- are relative permeability coefficients, from Hodgkin and Horowitz (12).

Under the situation where the cell membrane has significant permeability to both ionic and nonionic forms of ammonia, T_{Amm} distribution will be a function of both transmembrane pH and E_m gradients. According to Boron and Roos (2)

$$\frac{[T_{Amm}]_i}{[T_{Amm}]_e} = \frac{[H^+]_i + K}{[H^+]_e + K} \times \frac{(PNH_3/PNH_4^+) - F \times E_m/[RT(1 - \gamma)] \times [H^+]_e/K}{(PNH_3/PNH_4^+) - F \times E_m \times \gamma/[RT(1 - \gamma)] \times [H^+]_i/K} \quad (12)$$

where K is the NH_3/NH_4^+ dissociation constant, PNH_3 and PNH_4^+ are the permeabilities to NH_3 and NH_4^+ , respectively, and

$$\gamma = \exp\left(\frac{E_m F}{RT}\right) \quad (12)$$

If the pH_i gradient and the E_m are known, then the $[T_{Amm}]_i/[T_{Amm}]_e$ ratio will be a function of the permeability ratio PNH_3/PNH_4^+ as outlined by Wright et al. (38) and Wood et al. (37).

All data are reported as means \pm SE. Significant differences between means in the four different perfusate groups were evaluated by one-way analysis of variance (ANOVA). If the ANOVA indicated significance ($P \leq 0.05$), then post hoc comparison by means of Duncan's multiple-range and critical-range test ($P \leq 0.05$) was performed, with reference to the medium-pH group as the control. Student's paired t -test was used to evaluate differences within treatment groups between 30- and 60-min values. Simple unpaired t -tests were used to evaluate differences between the low- pH_e treatment and the low- pH_e plus amiloride treatment.

RESULTS

Condition of the Perfused Tail-Trunk Preparation

The perfusion pressure started at ~ 15 cmH $_2$ O and, thereafter, slowly declined by ~ 5 cmH $_2$ O as the perfusion proceeded for the first 30 min. However, this trend was reversed during the second 30 min, such that perfusion pressures at 60 min were 16–19 cmH $_2$ O.

Table 2. Net perfusion pressure after 30 and 60 min perfusion in the four experimental treatment groups

| | Low pH | Medium pH (Control) | High pH | High K^+ (Depolarized) |
|--------|-----------------|------------------------|-----------------|-----------------------------|
| 30 min | 10.3 \pm 1.1 | 11.6 \pm 1.0 | 11.1 \pm 1.4 | 8.7 \pm 0.9 |
| 60 min | 17.7 \pm 2.7* | 18.6 \pm 2.2* | 16.1 \pm 3.1* | 16.7 \pm 2.7* |
| n | 7 | 11 | 8 | 6 |

Values are means \pm SE for each treatment group (cmH $_2$ O). *Significantly different from corresponding 30 min values.

Table 3. $[H_2O]_t$, ICFV, and ECFV after 60 min of perfusion in the four experimental treatment groups

| | Low pH | Medium pH (Control) | High pH | High K ⁺ (Depolarized) |
|------------|-------------------|---------------------|-------------------|-----------------------------------|
| $[H_2O]_t$ | 0.795 ± 0.005 | 0.784 ± 0.001 | 0.779 ± 0.002 | 0.769 ± 0.009 |
| ICFV | 0.719 ± 0.005 | 0.703 ± 0.008 | 0.698 ± 0.008 | $0.735 \pm 0.012^*$ |
| ECFV | 0.076 ± 0.005 | 0.081 ± 0.008 | 0.080 ± 0.008 | $0.034 \pm 0.016^*$ |
| n | 7 | 11 | 8 | 6 |

Values are means \pm SE for each treatment group (ml/g wet tissue). $[H_2O]_t$, white muscle tissue water content; ICFV, intracellular fluid volume; ECFV, extracellular fluid volume. *Significantly different from corresponding control values.

There were no significant differences in pressure between the four groups at either 30 or 60 min (Table 2).

There was no visible red color in the outflow perfusate after 20 min of perfusion, indicating thorough washout of red blood cells. There were also no detectable differences in protein concentration ($\sim 3\%$) between inflowing and outflowing perfusate at any time. The $[H_2O]_t$ of each treatment group after 60 min perfusion (Table 3) was not significantly different from that of initial muscle samples (0.786 ± 0.016 ml/g wet tissue, $n = 32$, pooled total of 4 groups) and was, therefore, not affected by the experimental treatments. However, the high-K⁺ treatment caused a marked redistribution of internal fluid volumes, resulting in a 58% decrease in ECFV and a 5% increase in ICFV (Table 3). Similarly, white muscle ICF Na⁺, K⁺, and Cl⁻ showed no significant changes as pH_e varied, but Na⁺ and Cl⁻ were altered markedly in response to high-K⁺ perfusion (Table 4). ICF Na⁺ and Cl⁻ increased by 35 and 280%, respectively, relative to the control group, whereas K⁺ remained unchanged despite the large increase of ECF K⁺ (≈ 15 mM; Tables 4 and 5). It was not possible to compare these values with ICFV and ICF ion concentrations before perfusion because ECF measurements required for the intracellular calculations were not obtained when the initial muscle samples were collected. However, the ICFV and ECFV values of the three pH treatment groups, as well as the intracellular ionic concentrations after 60 min perfusion, were comparable to those of our previous in vivo study on exercised trout (29).

There were no significant differences of [Na⁺] or [Cl⁻] between inflow and outflow perfusate [arterial-venous (a-v) difference] in any of the three pH treatment groups after 60 min of perfusion (Table 5). Despite the

Table 4. Intracellular Na⁺, K⁺, and Cl⁻ concentrations in trout white muscle after 60 min of perfusion in the four experimental treatment groups

| | Low pH | Medium pH (Control) | High pH | High K ⁺ |
|---------------------------------|-----------------|---------------------|-----------------|---------------------|
| [Na ⁺] _i | 10.8 ± 0.7 | 15.6 ± 2.2 | 10.4 ± 2.0 | $21.0 \pm 0.9^*$ |
| [K ⁺] _i | 150.0 ± 3.6 | 160.8 ± 5.1 | 156.9 ± 3.7 | 150.5 ± 7.4 |
| [Cl ⁻] _i | 3.6 ± 0.2 | 3.3 ± 0.2 | 2.7 ± 0.1 | $12.5 \pm 0.9^*$ |
| n | 7 | 11 | 8 | 6 |

Values are means \pm SE for each treatment group (mmol/l ICF water). Subscript i, intracellular; brackets, concentration. *Significantly different from corresponding control values.

Table 5. Ionic concentrations (Na⁺, K⁺, and Cl⁻) in arterial and venous perfusate water after 60 min perfusion in the four experimental treatment groups

| | Low pH | Medium pH (Control) | High pH | High K ⁺ (Depolarized) |
|---------------------------------|-------------------|---------------------|-----------------|-----------------------------------|
| [Na ⁺] _a | 154.7 ± 8.8 | 165.8 ± 5.2 | 163.8 ± 5.9 | 142.8 ± 1.7 |
| [Na ⁺] _v | 154.5 ± 4.3 | 167.3 ± 4.2 | 163.1 ± 7.6 | 144.6 ± 0.8 |
| [K ⁺] _a | 3.08 ± 0.12 | 2.96 ± 0.16 | 2.94 ± 0.12 | 14.05 ± 0.71 |
| [K ⁺] _v | $3.65 \pm 0.22^*$ | $3.52 \pm 0.19^*$ | 3.29 ± 0.10 | $12.45 \pm 0.76^*$ |
| [Cl ⁻] _a | 153.4 ± 2.4 | 151.0 ± 3.3 | 128.7 ± 1.9 | 161.8 ± 2.3 |
| [Cl ⁻] _v | 148.4 ± 2.3 | 146.8 ± 1.6 | 130.5 ± 2.2 | 157.0 ± 1.4 |
| n | 7 | 11 | 8 | 6 |

Values are means \pm SE for each treatment group (mmol/l perfusate water). Subscript a and v, arterial and venous, respectively. *Significantly different from corresponding arterial values.

large increases in ICF [Na⁺] and [Cl⁻] in the high-K⁺ treatment, there were again no significant a-v differences in these two ions. However, [K⁺]_v increased by almost 20% relative to [K⁺]_a in both the low-pH_e and the medium-pH_e (control) groups, indicating a net efflux of K⁺ at 60 min (Table 5). This did not occur in the high-pH_e treatment. In contrast, the high-K⁺ group exhibited a 10% decline in [K⁺]_v relative to [K⁺]_a, indicating a net uptake of K⁺ at 60 min (Table 5). The trend for lower absolute ECF [Cl⁻] with increasing pH in the three pH treatments and the lower absolute ECF [Na⁺] in the high-K⁺ treatment was due to the original makeup of the salines (see MATERIALS AND METHODS).

E_m was not affected by perfusate acid-base status and averaged about -90 mV in the three pH treatments (Table 6). The increase in perfusate [K⁺] from 3 to 15 mM in the high-K⁺ treatment caused the intended partial depolarization (35%), reducing white muscle E_m to about -59 mV (Table 6). In this group, slight muscle twitching was observed at the start of perfusion with high-K⁺ saline. In all treatments, E_m remained unchanged when calculated with respect to either the arterial or venous ECF perfusate compositions (Table 6).

Typically, there was a 250- to 350-Torr decrease in P_{O₂} from the arterial to the venous perfusate, and O₂ uptake remained relatively stable over the course of perfusion in all four treatment groups (Table 7). The O₂ supply did not seem to be exhausted, because venous P_{O₂} (>75 Torr) was far from being depleted. O₂ uptake

Table 6. E_m in the four experimental treatment groups after 60 min perfusion, as estimated from the measured intra- and extracellular [Na⁺], [K⁺], and [Cl⁻], according to the Goldman-Hodgkin-Katz equation (Eq. 11)

| | Low pH | Medium pH (Control) | High pH | High K ⁺ (Depolarized) |
|----------|-----------------|---------------------|-----------------|-----------------------------------|
| Arterial | -89.9 ± 1.1 | -93.7 ± 1.6 | -91.5 ± 1.4 | $-58.8 \pm 2.0^*$ |
| Venous | -88.0 ± 1.6 | -91.8 ± 1.5 | -91.4 ± 1.0 | $-59.7 \pm 1.0^*$ |
| n | 7 | 11 | 8 | 6 |

Values are means \pm SE for each treatment group. E_m, transmembrane Nernst potential. E_m values calculated with respect to arterial inflow and venous outflow perfusate compositions are compared. *Significantly different from corresponding control value.

Table 7. In- and outflowing perfusate PO_2 , O_2 consumption, and CO_2 efflux rate of the tail-trunk preparation after 60 min perfusion

| | Low pH | Med pH (Control) | High pH | High K^+ (Depolarized) |
|--------------------------------------------------------------|--------------------|---------------------|-------------------|-----------------------------|
| PaO_2 , Torr | $321.4 \pm 24.0^*$ | 399.0 ± 16.3 | 413.8 ± 14.0 | 417 ± 5.95 |
| PvO_2 , Torr | 85.0 ± 10.4 | 115.6 ± 22.8 | 105.5 ± 12.1 | $74.0 \pm 7.4^*$ |
| MO_2 , mmol· kg ⁻¹ ·h ⁻¹ | $0.48 \pm 0.03^*$ | 0.60 ± 0.03 | 0.66 ± 0.03 | $0.73 \pm 0.02^*$ |
| CO_2 efflux, mmol· kg ⁻¹ ·h ⁻¹ | $1.45 \pm 0.02^*$ | 1.20 ± 0.15 | $0.69 \pm 0.23^*$ | 1.47 ± 0.14 |
| n | 7 | 11 | 8 | 6 |

Values are means \pm SE for each treatment group. MO_2 , oxygen consumption. *Significantly different from corresponding control values.

did not vary significantly among the three pH treatments, although it tended to be lower at reduced pH values. However, the high- K^+ group exhibited a 20% increase over the control group in O_2 consumption (Table 7).

CO_2 efflux was much greater than O_2 uptake, a difference that varied in accord with perfusate pH from 0.7-fold in the high-pH to 3-fold in the low-pH treatment (Table 7). Changes in pH altered CO_2 efflux significantly. Although low- pH_e treatment resulted in a 20% increase, the high- pH_e treatment led to a 70% depression in CO_2 efflux (Table 7). These data were in approximate inverse relation to the simultaneously measured metabolic acid flux data (Wang et al., unpublished results), suggesting that most of the CO_2 efflux occurred in the form of HCO_3^- .

Acid-Base Status

The intended differences in pH_a among treatments were achieved (Fig. 3, see Table 1), and nonbicarbonate buffer capacities (β) of perfusate used in the four treatment groups were not significantly different. The overall mean value was -5.54 ± 0.15 mM $[HCO_3^-]$ pH/unit. As arterial pH (pH_a) increased from 7.4 to 8.4, the a-v difference (ΔpH_{a-v}) also increased from 0.13 to 0.34 units (Fig. 3). However, the substantial differences in pH_a among treatments (~ 1.0 unit between high- and low-pH perfusates) had no effect on muscle pH_i , which remained at about 6.6 in this postexercise preparation. Therefore, the overall transmembrane pH gradient (ΔpH_{v-i}) varied linearly with pH_a , from 0.70 at low pH_a to 1.50 at high pH_a (Fig. 3). It should be noted that pH_i measured in initial muscle samples taken immediately before the start of perfusion was 6.596 ± 0.026 ($n = 30$) and therefore identical to the 6.6 measured after 60 min in the three pH treatments.

In contrast to the pH treatments, the 35% reduction of the muscle cell E_m induced by higher extracellular $[K^+]$ resulted in a significant depression in pH_i to ~ 6.4 (Fig. 3). However, the overall ΔpH_{v-i} (1.20) did not change in comparison to the control group ($\Delta pH_{v-i} = 1.16$). Venous pH also fell significantly, so ΔpH_{a-v} almost doubled relative to the control group.

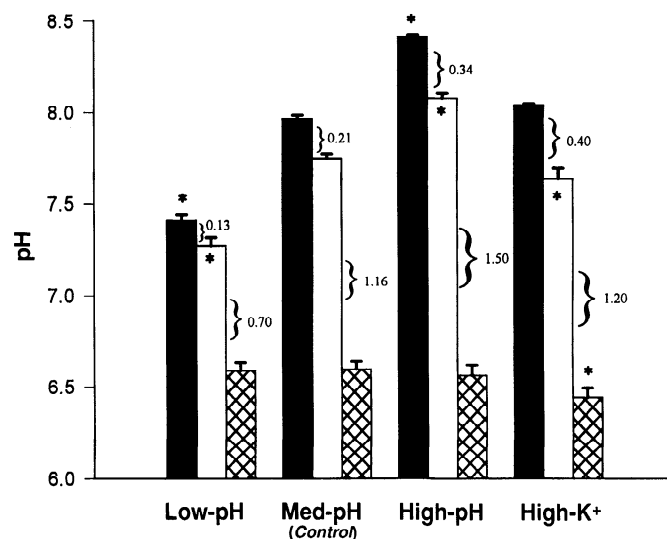


Fig. 3. pH in the inflowing saline [arterial (pH_a), solid bars], outflowing saline [venous (pH_v), open bars], and intracellular fluid (pH_i , crosshatched bars) of white muscle in 4 treatment groups of isolated-perfused tail-trunk preparations. Trunks were taken from trout exercised to exhaustion, and values were recorded after 60 min perfusion. Values are means \pm SE; $n = 7, 11, 8$, and 6 for the low-pH, medium-pH (control), high-pH, and high- K^+ groups, respectively. Braces indicate either a-v differences in pH or transmembrane pH gradients. *Significant difference ($P \leq 0.05$) from corresponding control value.

pH Effects on Ammonia Distribution and Efflux

Intracellular ammonia concentration (T_{Ammi}) was $\sim 9,000$ μM in this postexercise preparation, and there were no significant differences among the three pH treatment groups after 60 min of perfusion (Fig. 4). This may be compared with an initial value of $7,712 \pm 355$ μM ($n = 30$) measured in initial muscle samples taken before the start of perfusion. Thus there was a

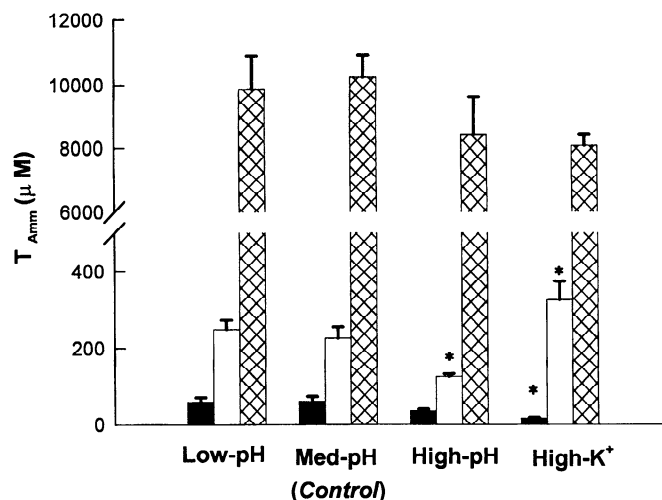


Fig. 4. $[T_{Am}]$ in inflowing saline [arterial (T_{Amma}), solid bars], outflowing saline [venous (T_{Ammv}), open bars], and intracellular fluid (T_{Ammi} , crosshatched bars) of white muscle in 4 treatment groups of isolated-perfused tail-trunk preparations. Trunks were taken from trout exercised to exhaustion, and values were recorded after 60 min perfusion. *Significant difference ($P \leq 0.05$) from corresponding control value.

small but significant increase in $T_{\text{Amm}i}$ over the course of the 60 min perfusion.

Compared with the control group, there was a 47% decrease in venous ammonia ($T_{\text{Amm}v}$) in the high- pH_e group but no significant change in $T_{\text{Amm}v}$ in the low- pH_e group (Fig. 4). In accord with the unchanged $T_{\text{Amm}i}$ and pH_i , there were no significant differences in intracellular P_{NH_3} among the three pH treatment groups; intracellular P_{NH_3} averaged ~ 150 μTorr (Fig. 5). Nevertheless, as extracellular pH increased, transmembrane P_{NH_3} gradients (intracellular to venous) dropped from 132.7 to 88.4 μTorr (Fig. 5). This depressed transmembrane P_{NH_3} gradient was mainly due to the elevation of venous P_{NH_3} induced by higher pH_e .

In parallel to the depressed transmembrane P_{NH_3} gradient, as pH_e increased, T_{Amm} efflux tended to decrease (Fig. 6). The high- pH_e treatment caused a significant 47% decrease in T_{Amm} efflux relative to the control group, whereas the 12% increase at low- pH_e was not significant (Fig. 6).

The measured transmembrane T_{Amm} ratio ($T_{\text{Amm}i}/T_{\text{Amm}e}$) was calculated relative to the venous end, a conservative approach maximizing the potential for equilibration. The ratio increased markedly as pH_e increased (Fig. 7). The lower venous T_{Amm} (Fig. 4) contributed primarily to the higher ratio. For comparison, the transmembrane pH gradients at the venous end were used to estimate the T_{Amm} distribution ratios (Eq. 9) assuming that the white muscle membrane is effectively permeable only to NH_3 . It is clear that T_{Amm} ratios calculated in this manner from the pH gradients were far from matching the measured ratios and indeed greatly underestimated them in all three pH treatment groups (Fig. 7). Nonetheless, as transmembrane pH gradient increased, the pH estimated ratio increased in parallel with the elevation in the measured T_{Amm} ratio

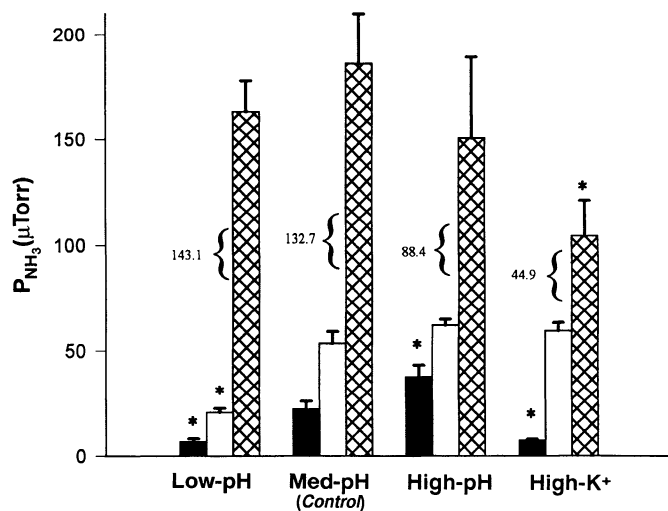


Fig. 5. Partial pressures of NH_3 (P_{NH_3} in inflowing perfusate (arterial, solid bars), outflowing perfusate [venous (P_{NH_3v}) open bars], and ICF (P_{NH_3i} , crosshatched bars) of white muscle in four treatment groups of isolated-perfused tail-trunk preparations. Braces indicate sizes of mean $\text{P}_{\text{NH}_3i} - \text{P}_{\text{NH}_3v}$ gradients. Trunks were taken from trout exercised to exhaustion, and values were recorded after 60 min perfusion. *Significant difference ($P \leq 0.05$) from corresponding control value. 70 $\mu\text{Torr} = 10$ mPa.

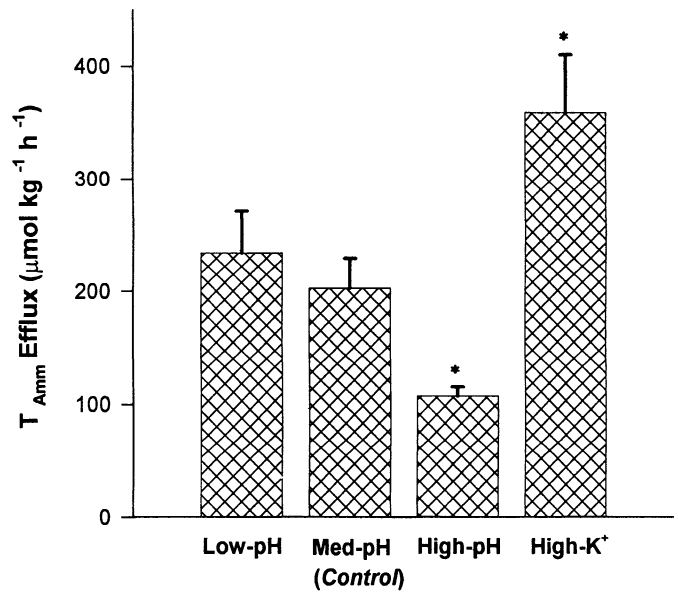


Fig. 6. T_{Amm} efflux from postexercise trout tail-trunk preparations after 60 min perfusion in 4 treatment groups. Efflux rates were expressed as $\mu\text{mol} \cdot \text{h}^{-1} \cdot \text{kg wet wt}^{-1}$ of tail-trunk. *Significant difference ($P \leq 0.05$) from corresponding control value.

(Fig. 7). The absolute differences between the measured and the pH estimated ratios remained almost unchanged as pH_e increased.

E_m Effects on Ammonia Distribution and Efflux

The membrane depolarization caused by the increase in extracellular K^+ did not alter $T_{\text{Amm}i}$ significantly (Fig. 4) but caused substantial elevations in both $T_{\text{Amm}v}$ (Fig. 4) and T_{Amm} efflux (Fig. 6) relative to the control

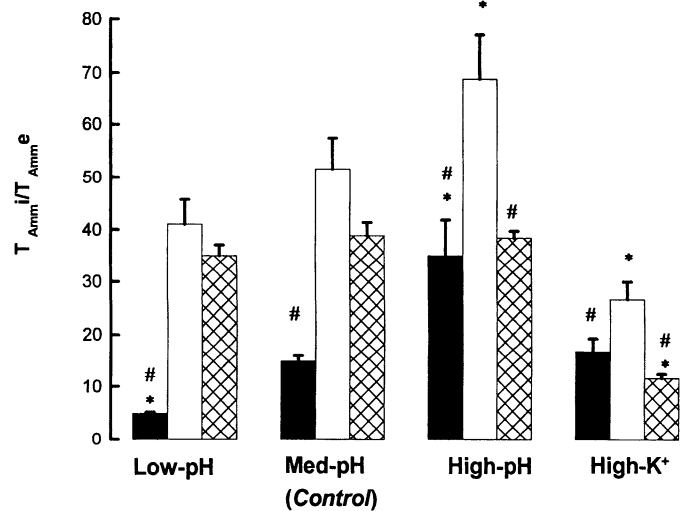


Fig. 7. Transmembrane distribution ratios of total ammonia ($T_{\text{Amm}i}/T_{\text{Amm}e}$) from intra- to extracellular fluid (venous outflowing perfusate) of white muscle in four treatment groups of isolated-perfused tail-trunk preparations. Measured values (open bars) are compared with values (solid bars) predicted from measured transmembrane pH gradients ($\Delta\text{pH}_{i,v}$) by Eq. 9, assuming permeability only to NH_3 and with values (crosshatched bars) predicted from E_m by Eq. 10, assuming permeability only to NH_4^+ . #Significant difference ($P \leq 0.05$) from corresponding measured ratio; * significant difference ($P \leq 0.05$) from corresponding ratios in medium-pH (control) group.

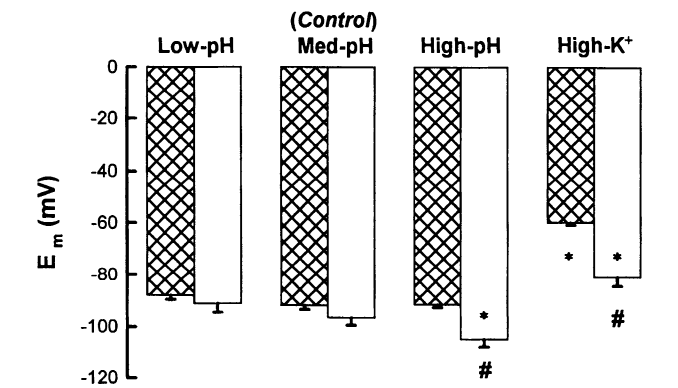


Fig. 8. Comparison between E_m estimated from measured intra- to extracellular K^+ , Na^+ , and Cl^- distributions by Eq. 11 (crosshatched bars) and Nernst potentials calculated from measured NH_4^+ distribution ratios by Eq. 10 (open bars) in 4 treatment groups of isolated-perfused tail-trunk preparations. *Significant difference ($P \leq 0.05$) from corresponding value in medium-pH (control) group; #significant difference ($P \leq 0.05$) from corresponding value estimated by Eq. 11.

group. This 77% increase in T_{Amm} efflux occurred despite a substantial fall in intracellular P_{NH_3} from ~170–100 μ Torr and an associated 64% decrease in transmembrane P_{NH_3} gradient (Fig. 5). The net driving force on NH_4^+ , calculated relative to the venous perfusate as the difference between the measured E_m and the Nernst E_m for NH_4^+ (from Eq. 10), increased more than threefold from 6.6 ± 2.6 ($n = 6$) to 20.1 ± 4.7 mV ($n = 11$).

For comparison, the values of E_m tabulated in Table 6 were used to estimate the T_{Amm} distribution ratios (Eq. 10) on the assumption that the white muscle cell membrane is effectively permeable only to NH_4^+ . Inasmuch as E_m did not vary significantly among the three pH treatments (Table 6), the E_m estimated T_{Amm}/T_{Ame} ratios did not change significantly (Fig. 7). In the low-pH_e and medium-pH_e (control) treatments, these E_m estimated ratios were not significantly different from the measured ratios. They therefore agreed much more closely with the measured ratios than did the pH estimated ratios (Fig. 7). However, in the high-pH_e treatment, the E_m estimated ratio and the pH estimated ratio were similar, and both were significantly lower than the measured ratio. Relative to the control group, the high- K^+ treatment caused a significant decrease in the measured T_{Amm} distribution ratio, which was paralleled by a significant decline in the E_m estimated ratio. In contrast, the pH estimated ratio increased slightly. In this case, the two estimated ratios were similar, and both were significantly lower than the measured ratio, similar to the situation at high pH (Fig. 7).

Table 8. Comparison of total ammonia distribution ratio across the white muscle cell membrane (intracellular to venous) and related parameters between the low pH and low pH plus amiloride (10^{-4} M) treatment groups

| Treatment Group | Ammonia Flux, $\mu\text{mol} \cdot \text{kg}^{-1} \cdot \text{h}^{-1}$ | Measured Ammonia Ratio | E_m Est Ammonia Ratio | pH Est Ammonia Ratio | ENH_4^+ , mV |
|------------------------------------|---------------------------------------------------------------------------|---------------------------|----------------------------|-------------------------|-------------------|
| Low pH ($n = 7$) | 228.37 ± 34.40 | 40.99 ± 4.64 | 35.12 ± 2.03 | 4.93 ± 0.26 | -91.14 ± 3.37 |
| Low pH plus amiloride ($n = 11$) | 251.26 ± 22.95 | 35.59 ± 3.16 | 40.12 ± 0.95 | 5.33 ± 0.28 | -88.66 ± 4.15 |

Values are means \pm SE for each treatment group. Est, estimated; ENH_4^+ , NH_4^+ distribution ratio estimated membrane potential. There were no significant differences ($P > 0.05$) in any parameters between the 2 groups.

To look at the matter from another perspective, Nernst potentials were calculated from the measured intra- and extracellular $[NH_4^+]$ concentrations on the assumption that the muscle cell membranes are permeable only to NH_4^+ (Eq. 10). The NH_4^+ estimated Nernst potentials agreed closely with recorded E_m values in the low-pH_e and medium-pH_e treatments, but were significantly more negative than E_m in the high-pH_e and high- K^+ treatments (Fig. 8). In general, these findings agree with the analysis based on distribution ratios (Fig. 7).

Amiloride Effects on Ammonia Distribution and Efflux

In general, the T_{Amm} distribution ratios predicted from E_m by Eq. 10, assuming that the white muscle cell membrane was effectively permeable only to NH_4^+ , agreed with the observed distribution ratios much better than did those predicted from pH gradients by Eq. 9, assuming effective permeability to NH_3 only (Fig. 7). This agreement was strongest in the low-pH_e treatment. We therefore evaluated whether amiloride (10^{-4} M), an inhibitor of both $Na^+/H^+-NH_4^+$ exchange and Na^+ channels at this concentration (1), influenced the distribution and efflux of ammonia in the low-pH_e treatment.

Amiloride had no significant effect on pH gradients or E_m in the preparation (data not shown). Amiloride also had no significant effect on either the measured T_{Amm} distribution ratio or the measured T_{Amm} efflux rate (Table 8).

DISCUSSION

Evaluation of the Tail-Trunk Perfusion Preparation: Comparison With in Vivo Studies

The present perfused trout trunk preparation is similar to that of Moen and Klungsoyr (18). In contrast to whole trunk preparations (16, 28, 33), only the postanus region of the tail was perfused, thereby avoiding involvement of the kidney and allowing discrete collection of venous outflow from the caudal vein. In this region, white muscle makes up ~90% of the total soft tissue volume (8), the balance being mainly red muscle in a discrete band under the lateral line. The preparation therefore facilitates the measurement of metabolite fluxes between white muscle and ECF, but cannot preclude small contributions from red muscle. The perfusion flow rate of $2 \text{ ml} \cdot \text{min}^{-1} \cdot 100 \text{ g tail wt}^{-1}$ was chosen as a compromise between O_2 delivery requirements and measurement accuracy for ΔT_{Amm} and other metabolites between inflow and out-

flow. This flow rate is about twice the blood flow rate to white muscle recorded during aerobic exercise in trout, or about three- to fourfold resting flow rates (23, 32). The only estimates of white muscle blood flow in trout after exhaustive exercise of the type used here are those of Neumann et al. (21), who reported a 1.5-fold increase from resting levels. Perfusion pressure was somewhat lower than in vivo levels, reflecting the absence of sympathetic tone in the preparation.

In preliminary tests, we found that the use of 3% BSA to provide colloid osmotic pressure was a major improvement relative to previous preparations employing polyvinylpyrrolidone or dextran as an oncotic agent (16, 18, 28, 33); vascular reactivity was sustained, edema did not occur, and the preparation exhibited fluid volumes and intracellular ion, pH, and T_{Amm} levels all comparable with those of our in vivo study on exhaustively exercised trout (29). The rate of MO_2 (Table 7) was ~25% of that measured in vivo on whole trout at rest or ~10% of that seen after exhaustive exercise (36). In view of the low metabolic rate of white muscle relative to aerobic tissues such as liver and gills, these figures seem quite reasonable. Certainly, the relatively high venous PO_2 (70–120 Torr; Table 7) indicated that O_2 supply was not compromised. In our preliminary tests, when the perfusion rate was reduced to one-third of the above rate or the arterial PO_2 was decreased to ~200 Torr, venous PO_2 could be depressed to as low as 10–20 Torr. This also suggests that the O_2 delivery to the preparation was far from insufficient.

Acid-Base Status

pH_i in the perfused trunk preparation (~6.6; Fig. 3) was very similar to that measured in the white muscle of exhaustively exercised trout in vivo and may be compared with resting values of ~7.2 both in vivo (25, 27, 29, 36) and in vitro (16). As extracellular “respiratory” acid-base status was maintained constant at a resting level of arterial PCO_2 in the postexercise tail-trunks, the acidotic pH_i was due to intracellular “metabolic acidosis” (low HCO_3^- , confirmed Wang et al., unpublished results). This was undoubtedly due to H^+ generation from lactate production and ATP breakdown during exercise as documented in many studies, such as those cited above. The significantly lower pH_i in the high- K^+ group was likely caused by additional muscle twitching induced by membrane depolarization; these trunks had higher intracellular lactate levels.

In the present experimental design, changes in extracellular acid-base status were achieved by purely “metabolic” adjustments (i.e., changes in HCO_3^-) at constant PCO_2 (Table 1), whereas in vivo after exhaustive exercise, both factors change: increased PCO_2 and decreased HCO_3^- . White muscle pH_i remained constant at the postexercise level independent of extracellular HCO_3^- and pH_e in both this in vitro study (Fig. 3) and in trout in vivo infused with a large dose of HCO_3^- after exhaustive exercise (27). These results suggest that metabolic acid-base disturbance in the ECF has minimal influence on intracellular acid-base status in white muscle, in contrast to the well-documented influence of ECF

respiratory acid-base disturbance on muscle pH_i both in vitro (16) and in vivo (35).

Ammonia Distribution and Efflux

Assuming that passive movements of NH_3 and NH_4^+ are the only routes by which ammonia can be released from muscle cells, then changes in P_{NH_3} gradients should dictate movements of the former, and changes in the net electrochemical gradients for NH_4^+ should dictate the latter. Our experimental design manipulated the former by changing pH_e (Fig. 3) and the latter by changing E_m (Table 6). The results show clearly that both factors had a significant influence on T_{Amm} efflux from the preparation. Thus, in the absence of changes in E_m (Table 6), T_{Amm} efflux decreased as pH_e increased (Fig. 6), and therefore the P_{NH_3} gradient decreased (Fig. 5). Conversely, T_{Amm} efflux increased with a partial depolarization by high K^+ (Fig. 6; Table 6), despite a marked reduction in the P_{NH_3} gradient. Specifically, a 47% decrease in efflux at high pH_e relative to medium pH_e was associated with an apparent 27% decrease in the P_{NH_3} gradient from ICF to venous perfusate. Conversely, a 77% increase in efflux in the high- K^+ treatment was associated with a 203% increase in the electrochemical gradient for NH_4^+ and a 67% decrease in the P_{NH_3} gradient. Although both NH_3 and NH_4^+ movements are clearly important, it is impossible to calculate the exact contribution of each component without knowledge of exactly how the gradients are distributed along the arterial to venous pathway in muscle capillaries and whether the absolute permeabilities change.

An alternative approach to the same general question is to examine the intracellular to extracellular distribution ratio of T_{Amm} (34, 37, 38), with the use of basic principles elaborated by Boron and Roos (2). With the use of Eq. 10, if PNH_4^+ predominates, then a relatively high $[\text{T}_{\text{Amm}}]_i/[\text{T}_{\text{Amm}}]_e$ dictated by E_m will result (see Fig. 1B); whereas if PNH_3 predominates, by Eq. 9, a relatively low $[\text{T}_{\text{Amm}}]_i/[\text{T}_{\text{Amm}}]_e$ dictated by the $\text{pH}_e\text{-pH}_i$ gradient will result (e.g., Fig. 1A). These ratios have fixed values for any fixed values of $\text{pH}_i\text{-pH}_e$ and E_m , but will change when $\text{pH}_i\text{-pH}_e$ and E_m vary. In the situation where both permeabilities are significant, the distribution ratio will be intermediate between the asymptotes set by $\text{pH}_i\text{-pH}_e$ (low value of the ratio) and by E_m (high value of ratio; see Fig. 1 of Ref. 34 for a graphical representation of the relationship). The exact value will be dictated by the exact value of $\text{PNH}_3/\text{PNH}_4^+$ as outlined in Eq. 12. In absolute terms PNH_4^+ does not have to quantitatively exceed PNH_3 for the distribution ratio to be dictated by E_m . Because there is so much more NH_4^+ than NH_3 in solution at physiological pH, even if PNH_4^+ is only 10% of PNH_3 (i.e., $\text{PNH}_3/\text{PNH}_4^+ \approx 10$), then the ratio will approach the asymptote dictated by E_m . It is important to note that this analysis assumes steady-state conditions and that all ammonia is freely diffusible.

Application of this approach to the present data set revealed several interesting features (Fig. 7). First, it

reinforces the conclusion that both the pH gradient, acting on NH_3 distribution, and E_m , acting on NH_4^+ distribution, are important in setting the distribution of T_{Amm} . Thus as pH_e increased at constant E_m , the measured distribution ratio increased in parallel to the pH-predicted distribution ratio. Conversely, as E_m was lowered by partial depolarization by high K^+ , the measured distribution ratio decreased in parallel to the E_m -predicted ratio. These changes occurred although the ratios predicted by the reciprocal controlling factors did not change significantly. Second, at least at low pH_e and medium pH_e , the observed ratios were not significantly different from the E_m -predicted values, but remained far above the pH-predicted values. Third, under all conditions, the measured distribution ratios were greater than the maximum ratios predicted by E_m , although these differences were only significant in the high- pH_e and high- K^+ treatments (Fig. 7). This situation precluded calculation of $\text{PNH}_3/\text{PNH}_4^+$ from Eq. 12.

This latter situation can only occur if steady-state conditions were not achieved and/or if some of the intracellular ammonia was not freely diffusible. Both explanations are possible. Although the tail-trunk was perfused for 1 h before measurements were made and calculation was based on the distribution ratios with respect to the venous outflow, it remains possible that disequilibrium persisted, especially if intracellular ammonia production was continuing. This is suggested by the fact that T_{Amm} actually increased over the 60 min of perfusion. Recent data (summarized in Fig. 9) from our study (R. Henry, Y. Wang, and C. M. Wood, unpublished results) on perfused tail-trunks from resting trout cast some light on the situation. In that investigation, ammonia released from resting trunks was negligible,

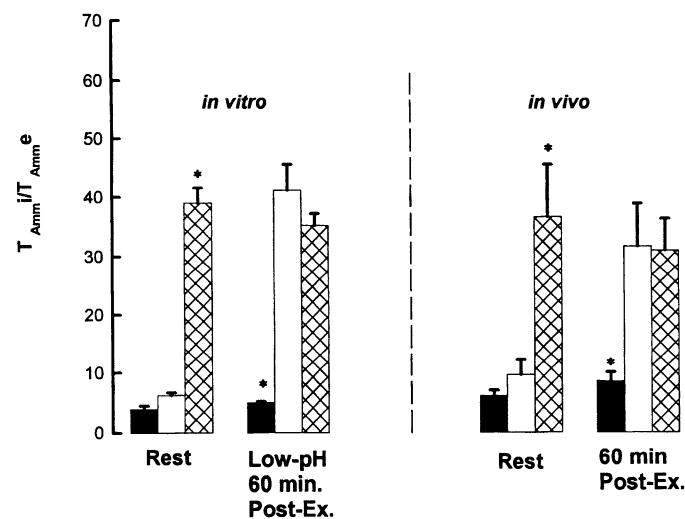


Fig. 9. Comparison of $T_{\text{Amm}i}/T_{\text{Amm}e}$ ratios across white muscle cell membranes *in vivo* (at rest and at 60 min postexercise) and *in vitro* in an isolated tail-trunk perfusion preparation (at rest and low- pH_e 60 min postexercise). Measured values (open bars) are compared with values (solid bars) predicted from measured transmembrane pH gradients by Eq. 9 and values (crosshatched bars) predicted from E_m (Eq. 10). *Significant difference ($P \leq 0.05$) from corresponding measured ratios. Resting *in vitro* data were obtained from a separate study (R. Henry, Y. Wang, and C. M. Wood, unpublished results). *In vivo* postexercise data were obtained from Wang et al. (29).

suggesting that production did not occur, and the measured distribution ratio was far below the maximum value predicted by E_m . Alternately or additionally, there is considerable evidence from mammalian studies that a portion of intracellular ammonia may be protein bound or otherwise compartmentalized (see Ref. 38 for a detailed discussion) and therefore not available for free diffusive exchange. An additional explanation might be that ammonia is actively transported into the ICF; however amiloride had no effect. Local pH gradients, which can be different from bulk gradients, may also complicate the analysis.

Amiloride was tested in the low- pH_e treatment where the observed distribution ratio most closely matched that expected from the effect of E_m on NH_4^+ . The complete lack of effect of this drug (Table 8) at a concentration (10^{-4} M) that should block both Na^+/H^+ - NH_4^+ exchangers and Na^+ channels (1) suggests that carrier mediation of this type is not involved in the movement of NH_4^+ across the white muscle cell membranes.

Comparison With *in Vivo* Studies

Overall, the present results indicating an ammonia distribution after exhaustive exercise close to that predicted by E_m , at least under the physiologically realistic condition of low pH_e , agree well with a number of investigations on exhaustively exercised teleost fish *in vivo* (27, 29, 38, 39). All of these studies have indicated that ammonia is distributed between white muscle ICF and ECF approximately according to E_m and not according to pH_e - pH_i after exercise; i.e., PNH_4^+ effectively predominates. Nevertheless, just as in the present study, artificially raising pH_e by HCO_3^- infusion after exhaustive exercise *in vivo* markedly increased the distribution ratio, inasmuch as more T_{Amm} accumulated in the ICF and less appeared in the blood plasma (27). Therefore, both *in vivo* and *in vitro*, PNH_4^+ is sufficiently large relative to PNH_3 after exhaustive exercise that ammonia distribution is largely governed by E_m acting on NH_4^+ . Nonetheless, PNH_3 is substantial, so ammonia efflux responds sensitively to the pH_e - pH_i gradient. These statements are not contradictory, for flux and distribution ratio are not the same quantity. Thus, in the dynamic postexercise situation at low pH_e , the Nernst potential for NH_4^+ is almost identical to E_m (Fig. 8), so there is no net driving force for NH_4^+ to leave the cells, but there is a large P_{NH_3} gradient for NH_3 to leave the cells (Fig. 5).

Under resting conditions, intracellular production of ammonia is presumably very small due to an absence of adenylate breakdown. Nevertheless, most *in vivo* studies on resting teleost fish have indicated that ammonia is again distributed according to E_m (27, 31, 38, 39). Under these conditions, the electrochemical gradient for inward movement of NH_4^+ would be balanced by the P_{NH_3} gradient for outward movement of NH_3 (Fig. 1B). Heisler (11) has objected to this conclusion on theoretical grounds, specifically that the resulting inward " H^+

shuttle" would place an intolerable load on the pH_i regulatory mechanisms of the cells.

Figure 9 illustrates that, in the perfused trout trunk under resting conditions (Henry et al., unpublished results) and in our recent in vivo study on trout (29), the $[T_{\text{Amm}}]_i/[T_{\text{Amm}}]_e$ distribution ratio was much lower than in all previous studies, far lower than that predicted by E_m and, in fact, approximated that predicted by $\text{pH}_e\text{-pH}_i$. The reason for the discrepancies between our resting data and those of many previous studies is unclear, but it should be noted that resting ratios are subject to the greatest error because of the low plasma T_{Amm} concentrations, the greatest bias because of arterial versus venous sampling, and the difficulty of obtaining muscle samples from resting fish without ammonia production from adenylate breakdown (30). These problems do not apply in the resting perfused trunk preparation.

The in vitro and in vivo patterns of Fig. 9 show remarkable agreement and suggest that the situation may change from a pH-dictated distribution at rest to an E_m -dictated distribution during recovery from exhaustive exercise. As pointed out earlier (29), the advantages of this switchover could be considerable. At rest, the costly H^+ shuttle would be avoided, whereas, after exercise, the E_m -dictated distribution would help retain much higher levels of ammonia in the muscle for greater intracellular buffering and ATP resynthesis. If this is the case, then the $\text{PNH}_3/\text{PNH}_4^+$ ratio of the white muscle cell membranes must decrease between rest and postexercise; acidosis itself might be a controlling factor.

We thank Dr. Scott D. Reid for making the schematic graph of the perfusion setup for us.

This study was supported by a National Science and Engineering Research Council operating grant to C. M. Wood and Medical Research Council grants to G. J. F. Heigenhauser. G. J. F. Heigenhauser is a Career Investigator for the Heart and Stroke Foundation of Ontario, Canada.

Present address and address for reprint requests: Y. Wang, Dept. of Zoology and Physiology, University of Wyoming, Laramie, WY 82071-3166.

Received 26 September 1995; accepted in final form 15 March 1996.

REFERENCES

- Benos, D. J. Amiloride: a molecular probe of sodium transport in tissue and cells. *Am. J. Physiol.* 242 (Cell Physiol. 11): C131-C145, 1982.
- Boron, W. F., and A. R. Roos. Comparison of microelectrode, DMO, and methylamine methods for measuring intracellular pH. *Am. J. Physiol.* 231: 799-809, 1976.
- Boutilier, R. G., T. A. Heming, and G. K. Iwama. Appendix: physicochemical parameters for use in fish respiratory physiology. In: *Fish Physiology*, edited by W. S. Hoar and D. J. Randall. New York: Academic, 1984, p. 403-430.
- Cameron, J. N., and N. Heisler. Studies of ammonia in the rainbow trout: physico-chemical parameters, acid-base behaviour and respiratory clearance. *J. Exp. Biol.* 105: 107-125, 1983.
- Conway, E. J. Nature and significance of concentration relations of potassium and sodium ions in skeletal muscle. *Physiol. Rev.* 37: 84-132, 1957.
- Dobson, G. P., and P. W. Hochachka. Role of glycolysis in adenylate depletion and repletion during work and recovery in teleost white muscle. *J. Exp. Biol.* 129: 125-140, 1987.
- Evans, D. H., and J. N. Cameron. Gill ammonia transport. *J. Exp. Zool.* 239: 17-23, 1986.
- Goolish, E. M. The scaling aerobic and anaerobic muscle powder in rainbow trout (*Salmo gairdneri*). *J. Exp. Biol.* 147: 493-505, 1989.
- Graham, T. E., J. Bangsbo, P. D. Gollnick, C. Juel, and B. Saltin. Ammonia metabolism during intense dynamic exercise and recovery in humans. *Am. J. Physiol.* 259 (Endocrinol. Metab. 22): E170-E176, 1990.
- Graham, T. E., J. W. E. Rush, and D. A. MacLean. Skeletal muscle amino acid metabolism and ammonia production during exercise. In: *Exercise Metabolism*, edited by M. Hargreaves. Champaign, IL: Human Kinetics, 1995, p. 131-175.
- Heisler, N. Mechanisms of ammonia elimination in fishes. In: *Animal Nutrition and Transport Processes 2. Transport, Respiration and Excretion: Comparative and Environmental Aspects*, edited by J. Truchot and B. Lahlou. Basel, Switzerland: Karger, 1990, p. 137-151.
- Hodgkin, A. L., and P. Horowitz. The influence of potassium and chloride ions on the membrane potential of single muscle fibres. *J. Physiol. Lond.* 148: 127-160, 1959.
- Jacobs, M. H., and D. R. Stewart. The distribution of penetrating ammonium salts between cells and their surroundings. *J. Cell. Comp. Physiol.* 7: 351-365, 1936.
- Kun, E., and E. B. Kearney. Ammonia. In: *Methods of Enzymatic Analysis*, edited by H. U. Bergmeyer. New York: Academic, 1971, p. 1802-1806.
- Meyer, R. A., G. A. Dudley, and R. L. Terjung. Ammonia and IMP in different skeletal muscle fibers after exercise in rats. *J. Appl. Physiol.* 49: 1037-1041, 1980.
- Milligan, C. L., and C. M. Wood. Intracellular pH transients in rainbow trout tissues measured by dimethadione distribution. *Am. J. Physiol.* 248 (Regulatory Integrative Comp. Physiol. 17): R668-R673, 1985.
- Milne, M. D., B. H. Scribner, and M. A. Crawford. Non-ionic diffusion and the excretion of weak acids and bases. *Am. J. Med.* 24: 709-729, 1958.
- Moen, K. A., and L. Klungsoyr. Metabolism of exogenous substrates in perfused hind parts of rainbow trout *Salmo gairdneri*. *Comp. Biochem. Physiol.* 68: 461-466, 1981.
- Mommsen, T. P., and P. W. Hochachka. The purine nucleotide cycle as two temporally separated metabolic units: a study on trout muscle. *Metabolism* 6: 552-556, 1988.
- Mutch, J. C., and E. W. Banister. Ammonia metabolism in exercise and fatigue: a review. *Med. Sci. Sports Exercise* 15: 41-50, 1983.
- Neumann, P., G. F. Holeton, and N. Heisler. Cardiac output and regional blood flow in gills and muscles after exhaustive exercise in rainbow trout (*Salmo gairdneri*). *J. Exp. Biol.* 105: 1-14, 1983.
- Pörtner, H. O., R. G. Boutilier, Y. Tang, and D. P. Toews. Determination of intracellular pH and PCO_2 after metabolic inhibition by fluoride and nitrilotriacetic acid. *Respir. Physiol.* 81: 255-274, 1990.
- Randall, D. J., and C. Daxboeck. Cardiovascular changes in the rainbow trout (*Salmo gairdneri* Richardson) during exercise. *Can. J. Zool.* 60: 1135-1140, 1982.
- Randall, D. J., and P. A. Wright. Ammonia distribution and excretion in fish. *Fish Physiol. Biochem.* 3: 107-120, 1987.
- Schulte, P. M., C. D. Moyes, and P. W. Hochachka. Integrating metabolic pathways in post-exercise recovery of white muscle. *J. Exp. Biol.* 166: 181-195, 1992.
- Tang, Y., and R. G. Boutilier. White muscle intracellular acid-base and lactate status following exhaustive exercise: a comparison between freshwater and seawater adapted rainbow trout. *J. Exp. Biol.* 156: 153-171, 1991.
- Tang, Y., H. Lin, and D. J. Randall. Compartmental distributions of carbon dioxide and ammonia in rainbow trout at rest and following exercise, and the effect of bicarbonate infusion. *J. Exp. Biol.* 169: 235-249, 1992.
- Turner, J. D., and C. M. Wood. Factors affecting lactate and proton efflux from pre-exercised, isolated-perfused rainbow trout trunks. *J. Exp. Biol.* 105: 395-401, 1983.

29. **Wang, Y., G. J. F. Heigenhauser, and C. M. Wood.** Integrated responses to exhaustive exercise and recovery in rainbow trout white muscle: acid-base, phosphogen, carbohydrate, lipid, ammonia, fluid volume and electrolyte metabolism. *J. Exp. Biol.* 195: 237–258, 1994.
30. **Wang, Y., M. P. Wilkie, G. J. F. Heigenhauser, and C. M. Wood.** The analysis of metabolites in rainbow trout white muscle: a comparison of different sampling and processing methods. *J. Fish Biol.* 45: 855–873, 1994.
31. **Wilkie, M. P., and C. M. Wood.** Recovery from high pH exposure in the rainbow trout: white muscle ammonia storage, ammonia washout, and restoration of blood chemistry. *Physiol. Zool.* 68: 379–401, 1995.
32. **Wilson, R. W., and S. Egginton.** Assessment of maximum sustainable swimming performance in rainbow trout (*Oncorhynchus mykiss*). *J. Exp. Biol.* 192: 299–305, 1994.
33. **Wood, C. M.** Pharmacological properties of the adrenergic receptors regulating systemic vascular resistance in the rainbow trout. *J. Comp. Physiol.* 107: 221–228, 1976.
34. **Wood, C. M.** Ammonia and urea metabolism and excretion. In: *The Physiology of Fishes*, edited by D. H. Evans. Boca Raton, FL: CRC, 1993, p. 379–425.
35. **Wood, C. M., and J. LeMoigne.** Intracellular acid-base responses to environmental hyperoxia and normoxic recovery in rainbow trout. *Respir. Physiol.* 86: 91–113, 1991.
36. **Wood, C. M., and R. S. Munger.** Carbonic anhydrase injection provides evidence for the role of blood acid-base status in stimulating ventilation after exhaustive exercise in rainbow trout. *J. Exp. Biol.* 194: 225–253, 1994.
37. **Wood, C. M., R. S. Munger, and D. P. Toews.** Ammonia, urea and H^+ distribution and the evolution of ureotelism in amphibians. *J. Exp. Biol.* 144: 215–233, 1989.
38. **Wright, P. A., D. J. Randall, and C. M. Wood.** The distribution of ammonia and H^+ between tissue compartments in lemon sole (*Parophrys vetulus*) at rest, during hypercapnia and following exercise. *J. Exp. Biol.* 136: 149–175, 1988.
39. **Wright, P. A., and C. M. Wood.** Muscle ammonia stores are not determined by pH gradients. *Fish Physiol. Biochem.* 5: 159–162, 1988.

